MECHANICAL PROPERTIES OF AN ULTRAFINE GRAINED C-MN STEEL

Rongjie Song;   Dirk Ponge;   Dierk Raabe
Max-Planck-Institut für Eisenforschung, Max-Planck-Str. 1, 40237 Düsseldorf, Germany

ABSTRACT

The mechanical properties of an ultrafine grained 0.2%C–Mn steel, processed by large strain warm deformation and subsequent annealing, have been investigated. The microstructure consists of spheroidized cementite particles in an ultrafine ferrite matrix (average grain diameter ≈ 1.3 µm). The steel shows an improved combination of strength and toughness when compared with corresponding coarse grained specimens. The reasonable ductility of the steel can be attributed to finely dispersed cementite particles which effectively increase the work hardening rate by the accumulation of geometrically necessary dislocations in their vicinity. The lower shelf energy is significantly higher and the ductile-to-brittle transition temperature is lower in the ultrafine grained steel than in the comparable coarse grained specimens. This may be due to the joint effect of grain refinement and delaminations in the ultrafine grained steel processed by the large strain deformation. The delaminations lead to a decrease in triaxiality of the stress state in the impact test samples. The upper shelf energy is slightly reduced in the ultrafine grained steel, which can be attributed to the effect of delamination.

KEYWORDS

Ultrafine grained steel; mechanical properties; ductility; toughness; shelf energy

INTRODUCTION

Among different strengthening mechanisms, grain refinement is the only method to improve both strength and toughness of materials simultaneously. This makes ultrafine grained materials very attractive. However, the ductility (elongation to failure observed in uniaxial tensile testing at room temperature) is severely reduced in ultrafine grained especially single phase steels with a grain size of about 1 µm when compare with corresponding coarse grained counterparts which typically have a grain size of about 10 µm. The sudden drop in uniform elongation in ultrafine grained steels is accompanied by a high yield ratio of approximately 1.0. Producing ultrafine grained steels with very high strength is increasingly feasible but strength alone is insufficient for many applications if the material does not provide sufficient ductility.

While several reports presented tensile properties of ultrafine grained steels [1–4], corresponding Charpy impact properties were rarely investigated due to limitations in sample size typically available from such laboratory-scale process set-ups.

In this study, the mechanical properties of an ultrafine grained 0.2%C–Mn steel produced by large strain warm deformation and annealing were investigated. The data are compared with the mechanical properties of a coarse grained steel with the same composition.

The goal of this study is twofold. First, we aim to obtain a better understanding of the insufficient work hardening rate in ultrafine grained steels, and to use this knowledge to improve the work hardening rate by introducing small spheroidized cementite particles in a fine ferrite matrix. Second, in order to study the Charpy impact properties of ultrafine grained steel, which was rarely studied in previous investigations, large samples of ~10 mm in thickness were produced by large-scale plane strain compression tests at the Max-Planck-Institut für Eisenforschung. The Charpy impact properties of the ultrafine grained steel, such as the low ductile-to-brittle transition temperature, are discussed in detail.

EXPERIMENTAL METHODS

Specimen preparation and experiments

The chemical composition of the C–Mn steel used in this work was 0.22C–0.21Si–0.74Mn–0.004P–0.003S–0.001N–0.029Al (mass%). The laboratory samples were machined directly from the cast ingot into rectangular parallelepiped samples of 50 × 40 × 60 mm^3 (width × length × height). The plane strain compression tests were conducted by use of a large scale 2.5 MN hot press [5], where the compression direction was parallel to the sample height.

After reheating with a heating rate of 10 K/s, the samples were austenitized at 1193 K for 3 minutes. After air cooling to 1143 K, a one-step deformation pass was exerted imposing a logarithmic strain of $\varepsilon = 0.3$ at a strain rate of 10 s^{-1}. This was followed by a controlled cooling procedure down to the pearlite finish temperature of 823 K at a cooling rate of 6.5 K/s. After this primary treatment which was identical for all specimens, the following different experimental routes were carried out to provide sets of different sample states:

a) Ultrafine grain route: After a 2 minutes holding period at 823 K, the large strain warm deformation was performed by applying a four-pass plane strain compression process with an inter-pass time of 0.5 s. Each of the four subsequent steps imposed a logarithmic strain of $\varepsilon = 0.4$ accumulating to a total strain of $\varepsilon = 1.6$. Each pass was conducted at a strain rate of 10 s^{-1}. Subsequently, an annealing treatment of 2 hours at 823 K was exerted.

b) Conventional route: After the controlled cooling and 2 min holding period at 823 K as described above the samples were water quenched in order to obtain a bainite–free ferrite–pearlite microstructure.

Characterization of microstructure

The microstructure characteristics of the specimens were investigated by use of light optical microscopy and high resolution scanning electron microscopy (SEM).

Measurement of the mechanical properties

Quasi-static mechanical characterization was conducted by using tensile test specimens with a round cross section (∅ = 5 mm) and with a gauge length of 25 mm. Tensile tests were conducted at room temperature with a constant cross–head speed of 0.5 mm/min.

Subsize Charpy V-notched specimens with a ligament size of 3 × 4 mm^2 were machined along the rolling direction according to the German Industry Norm DIN 50 115. Impact tests were conducted in a temperature range from 103 to 423 K. The value of the ductile-to-brittle transition temperature

HOME

(DBTT) was determined from the Charpy curve as the temperature corresponding to the half value of the upper shelf energy.

EXPERIMENTAL RESULTS

Microstructures obtained from the conventional and ultrafine grain routes

The microstructure of the steel after the conventional route consists of ferrite and pearlite (Fig. 1a). After the large strain warm deformation (ε = 1.6) and subsequent annealing at 823 K for 2 h (ultrafine grain route), the microstructure consists of ferrite with a small grain size and globular cementite particles (Fig. 1b). The average ferrite grain sizes in the initial ferrite–pearlite microstructure (Fig. 1a) and in the ultrafine microstructure (Fig. 1b) are 6.8 µm and 1.3 µm, respectively. Further details of the microstructure were reported earlier in [6].

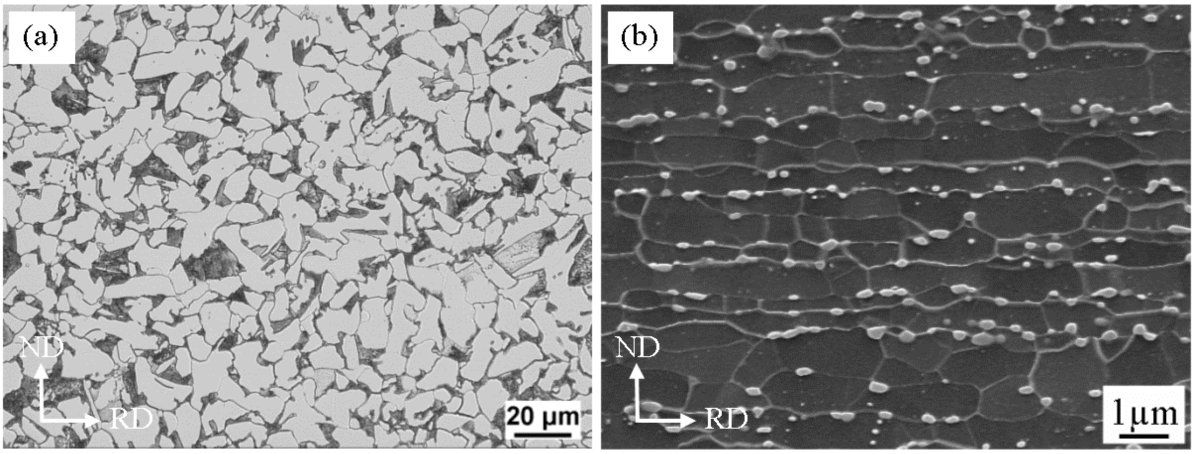

Fig. 1 (a) Light optical micrograph of the initial ferrite– pearlite microstructure of the steel processed by the conventional route; (b) SEM image of the ultrafine grained steel processed by the ultrafine grain route.

Comparison of the mechanical properties between the conventional and the ultrafine grained steels

Fig. 2 shows the tensile properties of the conventional and the ultrafine grained steels at room temperature. The decrease in grain size from 6.8 µm to 1.3 µm leads to an increase in strength (especially of the lower yield stress) and Lüders strain. The ductility of the ultrafine grained steel decreases. The total elongation yields about 20%.

Charpy impact properties

Fig. 3 shows the impact transition curves of the steels for subsize specimens. Compared with the conventional steel the upper shelf energy is decreased and the sigmoidal curve is more flat in the ultrafine grained steel. As introduced above, the ductile-to-brittle transition temperature is defined as the temperature at the half of the upper shelf energy. Fig. 3 shows that the decrease in grain size leads to a decrease in the ductile-to-brittle transition temperature. In the ductile-to-brittle transition region the absorbed energy changes slightly with temperature for the ultrafine grained steel.

HOME

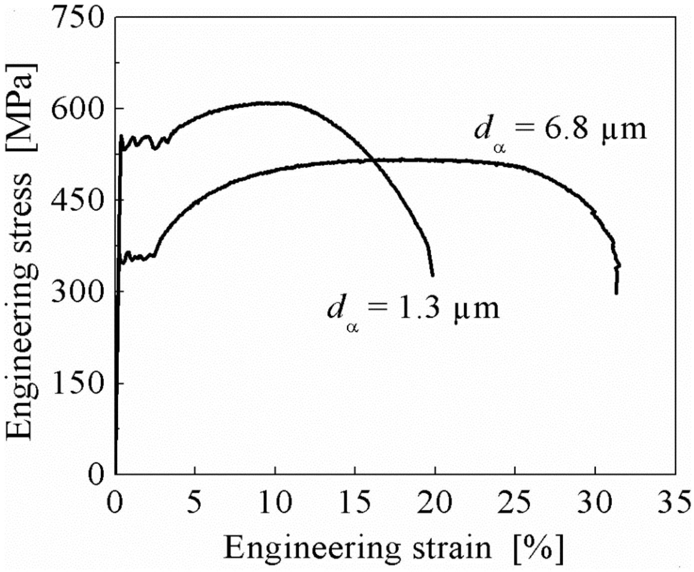

Fig. 2 Comparison of engineering stress–strain curves of the steels with different ferrite grain sizes. The different grain sizes were produced by the conventional route and the ultrafine grain route, respectively. The symbol d_α refers to the average ferrite grain diameter.

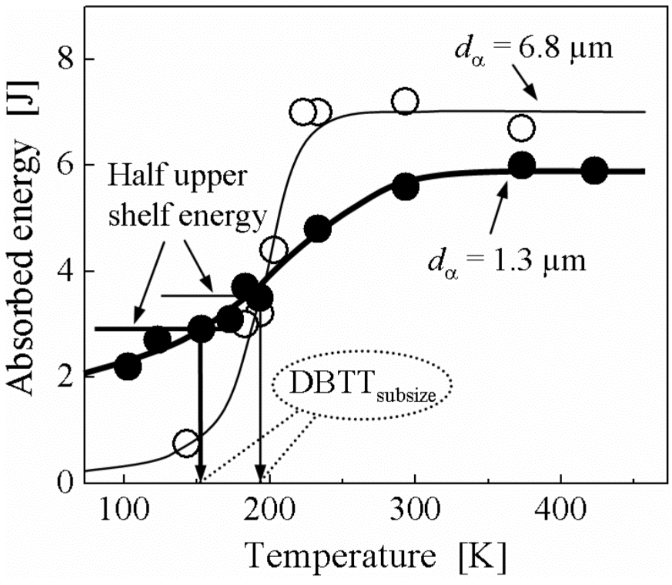

Fig. 3 Change of Charpy impact properties of the steels with different ferrite grain sizes. $DBTT_{subsize}$: ductile-to- brittle transition temperature of subsize specimen with a ligament size of 3 × 4 mm^2.

It is important to note that the lower shelf energy of the ultrafine grained steel is much higher than that of the conventional steel. Figs. 4a and b show the fracture surfaces of the ultrafine grained steel and the conventional steel tested at 103 K and 143 K, respectively. In Fig. 4a, the fracture surface of the ultrafine grained steel consists of both, smooth delaminations and dimpled fracture, in alternating sequence. Nearly 50% shear fracture can be observed in the fracture surface. In contrast to the ultrafine grained specimen, in the conventional steel cleavage fracture (nearly 100%) occurs already at 143 K, Fig. 4b.

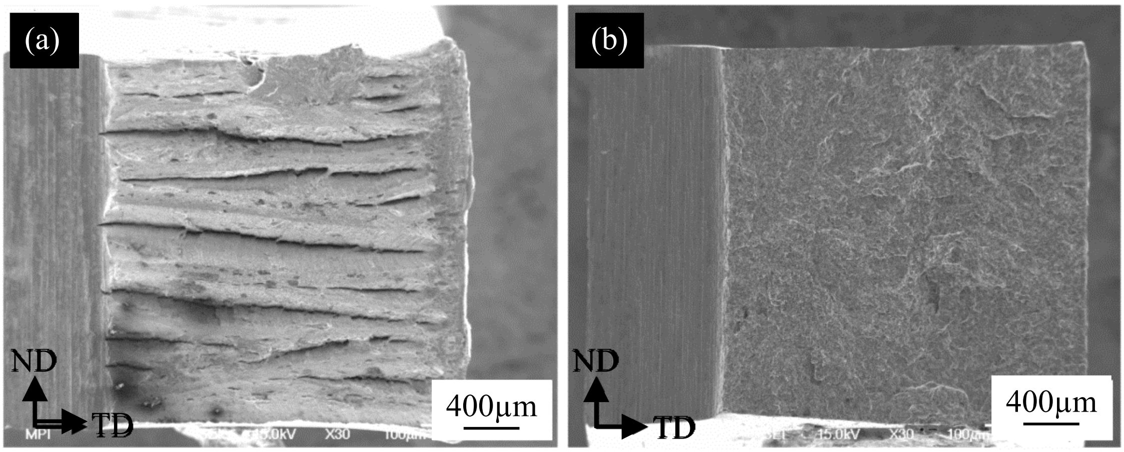

Fig. 4 SEM micrographs of the fracture surfaces for the steels with different ferrite grain sizes after Charpy impact tests. (a) Fracture surface of the ultrafine grained steel after impact testing at 103 K; (b) Fracture surface of the conventional steel after impact testing at 143 K.

Fig. 5a shows the SEM image of the ultrafine grained steel after the Charpy impact test at 103 K (Fig. 4a) but measured this time in the transverse direction of the specimen. The serrated area of the sample close to the fracture surface (Fig. 5a) displays the alternating ductile and delaminated areas of the facture surface (Fig. 4a). The white arrows in Fig. 5a point out chains of large voids in the specimen in front of the actual fracture surface, which are aligned parallel to RD. Figs. 5b and c show large magnifications of the crack along RD and the area below a shear surface, respectively, in terms of microtexture maps taken by EBSD. The orientation maps show the crystalline directions parallel to ND as indicated by the colors in the stereographic triangle, Fig. 5c. Fig. 5b shows mainly two colors at the tip of the crack, namely, red and blue indicating the texture components of <111> || ND (in blue) and <001> || ND (in red). It can be seen that the crack separates the elongated clusters of grains with different texture components of <111> || ND and <001> || ND, which demonstrate that the crack spreads along the boundaries of the grains (e.g. grain “1” and “2”) with different orientations. Fig. 5c shows the ND orientation map below a shear fracture.

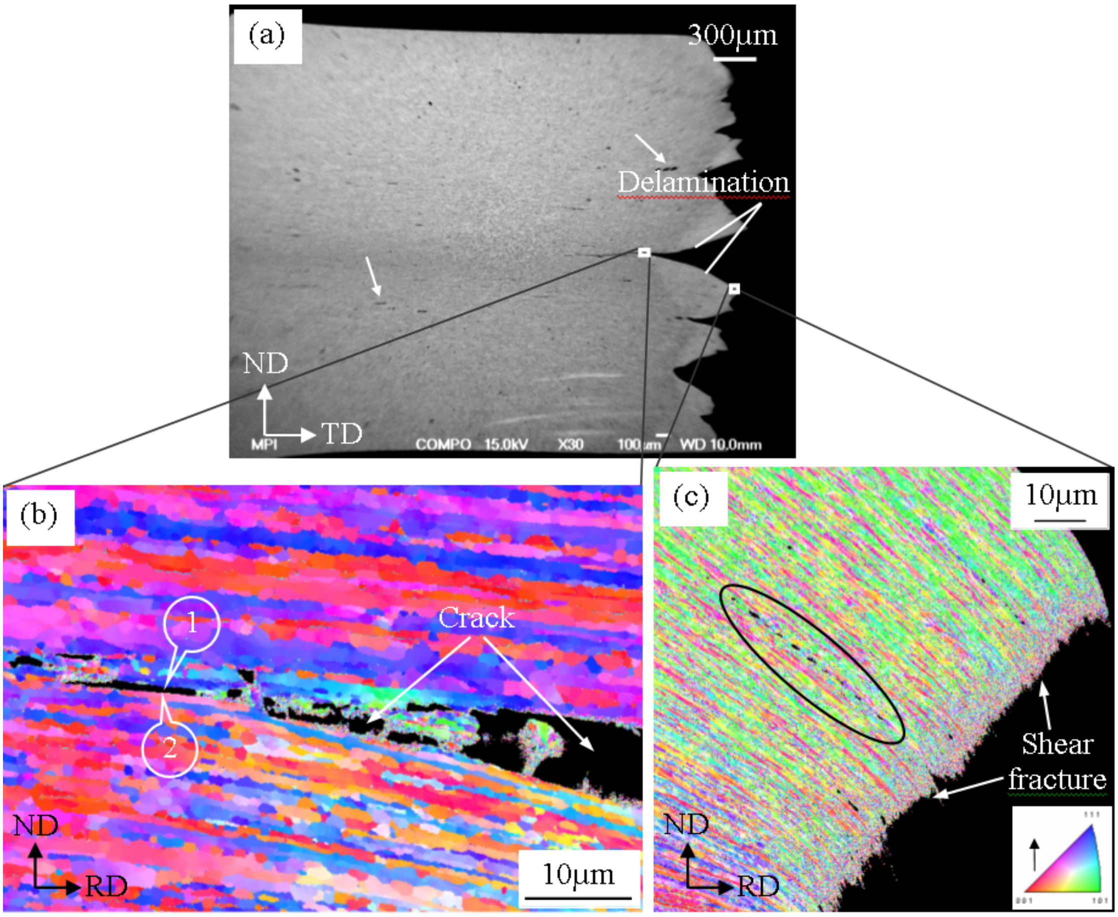

Fig. 5 SEM image and ND orientation maps (taken by the EBSD measurement) of the ultrafine grained steel after Charpy impact testing at 103 K, the same specimen as shown in Fig. 5a but measured in the transverse direction (TD) of the sample. (a) Total view of the sample in TD; (b) Front of a crack; (c) Aligned damage below a shear fracture.

DISCUSSION

Tensile properties

Compared with the tensile properties of the conventional steel, a substantial enhancement of strength is found for the ultrafine grained steel, Fig. 2. Numerous investigations have shown that grain refinement leads to an increase in strength.

One of the unusual aspects of ultrafine grained steels is their relatively low tensile ductility at room temperature (especially the uniform elongation) compared with their coarse-grained counterparts. This applies also in the current case. The data shown in Fig. 2 indicate that the work hardening is reduced by grain refinement. This is reflected by a higher yield ratio (lower yield stress/ultimate tensile stress) of about 0.9 for the ultrafine grained steel compared with a ratio of 0.7 for the conventional steel. The reason for the decrease in tensile ductility at room temperature for the ultrafine grained steel can be explained as follows:

First, *dynamic recovery* as a softening mechanism is able to reduce the apparent work hardening rate. During tensile deformation, dislocations which carry the intragranular strain are trapped at grain boundaries. Especially in ultrafine grained steels, the kinetics of dynamic recovery is associated with the spreading of trapped lattice dislocations into grain boundaries [8−9]. This decrease in dislocation density leads to no significant accumulation of dislocations inside the grains and, consequently, to less work hardening when compared with corresponding steels with large grain size. Following these earlier investigations, we assume that there are two kinds of recovery mechanisms, namely, *slow recovery in the grain interior* and *much fast recovery in the vicinity of* *grain boundaries*. In coarse grained steels the later one was not clearly observed due to a lower volume fraction of the overall volume near grain boundaries.

The reduced work hardening rate favors plastic instability. The decrease in tensile ductility can be explained in terms of *plastic instabilities*, which initiate necking due to excessive localized deformation [4].

The yield ratio is high in ultrafine grained steel, Fig. 2. However, apart from the high strength a good ductility can still be obtained, as is documented by the total elongation of about 20% and the uniform elongation of about 10%, Fig. 2. These values are different from the results reported in previous studies which presented total elongations of not more than 10%. The good ductility in the present case can be attributed to the presence of finely dispersed cementite particles which improve the work hardening capacity [4]. A large volume fraction and a fine dispersion of the cementite particles effectively increases the work hardening rate by promoting the accumulation of geometrically necessary dislocations around the particles [10].

In Fig. 2 the decrease in grain size leads to an increase in the Lüders strain. These phenomena can be linked to an instantaneous low density of mobile dislocations, the lack of dislocation sources within the grains, and the low work hardening rate of ultrafine grained alloys. A decrease in the work hardening rate in the ultrafine grained steel, which may be attributed to the rapid dynamic recovery, leads to stress saturation in a large strain interval. This amounts to slow propagation of the Lüders band front for the steel with a fine microstructure.

Toughness

Fig. 3 shows that the lower shelf energy is significantly higher in the ultrafine grained steel than in the coarse grained steel. On the one hand, this can be attributed to the effect of grain refinement on improving toughness even at very low temperatures. On the other hand, this phenomenon can be related to the anisotropic microstructure or pronounced crystallographic texture of the ultrafine grained steel produced by large strain deformation below the A_1 temperature (austenite to pearlite transformation finish temperature).

After the large strain deformation, a strong alignment of the microstructure was formed along the rolling direction, Fig. 4a. In Fig. 5a the chains of voids along RD were visible. A large magnification of the crack tip, Fig. 5b, showed that the path of crack propagation was located between two elongated grains with different texture components of <111> || ND and <001> || ND, respectively, which were separated by a high–angle grain boundary (i.e. grain “1” and grain “2”). This observation demonstrates that a high–angle grain boundary acts as a favorable path for crack propagation. This is more preferred in the case of large cementite particles locating at ferrite grain boundaries, e.g. the alignment of voids along the grain boundaries in Fig. 5c. The alternating microstructure of ferrite and aligned cementite particles facilitates the spread of cracks (below the V-notch) not only in the transverse direction but also in the rolling direction, Figs. 4a, 5a and b.

Fig. 3 shows a lower specific upper shelf energy in the ultrafine grained steel if compared with the conventional steel. On the one hand, this may be due to the relatively low ductility in this steel, which is documented by the smaller integrated area below the engineering stress–strain curve before necking, Fig. 2. Another reason can be attributed to the appearance of some delaminations in the ultrafine grained steel tested even in the upper shelf region [11].

According to [12], the phenomenon of delamination does not have influence on crack growth speed in ductile failure. Nevertheless, delamination leads to a reduction of the ductile-to-brittle transition temperature, which may be mainly due to the anisotropic microstructure resulted from large strain deformation. However, the large strain deformation at low deformation temperature is a favorable method currently to produce ultrafine grained microstructure. Therefore, it might be particularly attractive in the future projects to develop ultrafine grained steels by use of relatively low strain and high temperature.

CONCLUSIONS

An excellent combination of strength and toughness was obtained in an ultrafine grained 0.2%C–Mn steel produced by large strain warm deformation. A significant work hardening led to a reasonable ductility in the ultrafine grained steel, which is documented by about 10% uniform elongation and 20% total elongation. Grain refinement also resulted in an increased Lüders strain.

The lower shelf energy was significantly raised and the ductile-to-brittle transition temperature was lower in the ultrafine grained steel if compared to the coarse grained steel. This was attributed to the joint effect of the small ferrite grain size and the occurrence of delamination, which entailed a decrease in the triaxiality of the stress state in the impact test sample of the ultrafine grained steel.

REFERENCES

1) P.D. Hodgson, M.R. HICKSON and R.K. GIBBS, Scripta Mater. 40; (1999), p.1179.
2) R. SONG, R. KASPAR, D. PONGE and D. RAABE, Ultrafine Grained Materials III,TMS 2004, North Carolina,USA (2004), p 445.
3) R. SONG, D. PONGE and R. KASPAR, Steel Research 75, (2004), p.33..
4) R. SONG, D. PONGE and D. RAABE, Scripta Mate. 52, (2005), p.1075.
5) R. KASPAR and O. PAWELSKI, Materialprüfung 31, (1989), p.14.
6) R. SONG, D. PONGE, D. RAABE and R. KASPAR, Acta Mater. 53, (2005), p.845.
7) R. Kaspar and H. FAUL, MP Materialprüfung 43, (2001), p.18.
8) R.Z. Valiev, E.V.KOZLOV, Y.F. IVANOV, J. LIAN, A.A. NAZAROV and B. BAUDELET, Acta Metall. et Mater. 42, (1994), p.2467.
9) W. Lojkowski, Acta Metall. et Mater. 39, (1991), p.1891.
10) M.F. Ashby, Philos. Mag. 21, (1970), p.399.
11) R. SONG, D. PONGE and D. RAABE, submitted to Acta Mater..
12) E. Miyoshi, M. Fukuda, H. Iwanaga and T. Okazawa, Proc. Inst. Of Gas Eng. Conf., Crack Propogation in Pipe Lines (1974), paper 4.